

The Correlation Between Lightning and DSD Parameters

John R. Saylor, Carl W. Ulbrich, James W. Ballentine, and Justin L. Lapp

Abstract—The number of lightning strokes that struck a fixed region about the Clemson Atmospheric Research Laboratory (CARL) in Clemson, SC were recorded. These were correlated to characteristics of the drop size distribution (DSD). The DSD was parameterized in the usual way, using a two-parameter exponential function, where the two parameters are Λ and N_0 . The results showed that a power law fit adequately correlates both Λ and N_0 to the number of lightning strokes per hour per square mile. A linear fit performs poorly in this regard. The results also showed that the rain rate R was well-correlated to the number of lightning strokes per hour per square mile if a power law fit is employed. The use of lightning flash polarity was not found to be useful in relating R to lightning. These results are used to develop an understanding of the relationship between drop size statistics and lightning characteristics. The future utility of these findings to the remote sensing of rain rate is discussed.

Index Terms—Drop size distribution (DSD), lightning, precipitation, rain.

I. INTRODUCTION

LAND-BASED radar is currently the most effective method for continuous measurement of rainfall over large areas. Excellent precipitation radar coverage can be found in places such as the U.S. However, in other locations radar coverage is poor, and alternative methods for measuring rain remotely are needed. Lightning has been proposed as a possible measure of rain rate R in regions where radar coverage is lacking (e.g., Tapia *et al.* [1]). Cloud-to-ground lightning flashes can be measured remotely via ground-based detection networks such as the National Lightning Detection Network (NLDN). More localized networks also exist, such as the Los Alamos Sferic Array (LASA) [2] and the New Mexico Tech Lightning Mapping Array (LMA) [3]. Satellite resources are available in addition to these ground-based networks. For example, from 1995 to 2000, lightning strike information was obtained by the Optical Transient Detector (OTD) aboard the MicroLab-1 satellite, which provided global coverage [4]. The Lightning Imaging Sensor (LIS) [5], [6] aboard the Tropical Rainfall Measuring Mission (TRMM) satellite [7], [8] has provided information on lightning strikes in the tropics from 1998 to the present. Plans for placing a lightning mapper on future geostationary satellites have also been put forth at various times [9], [10]. Hence, an algorithm capable of relating some characteristic of lightning to rain rate R has the potential of enhancing the remote measurement of rain.

Manuscript received September 17, 2004; revised March 17, 2005. This work was supported in part by the National Aeronautics and Space Administration and in part by the National Science Foundation.

The authors are with the Department of Mechanical Engineering, Clemson University, Clemson, SC 29634 USA (e-mail: jrsaylor@ces.clemson.edu).

Digital Object Identifier 10.1109/TGRS.2005.851638

Several investigations have been performed seeking to correlate the number of cloud-to-ground lightning flashes to R (or one of several variables related to R). A survey of some of these studies is presented below. A more detailed review can be found in a paper by Petersen and Rutledge [11].

In this work, the following terminology will be used. A lightning “flash” will refer to a lightning event that occurs over a relatively brief interval of time (<1 s) and consists of lightning discharges occurring along the same nominal ionization channel (resulting in ground strike locations within about 1 km). A lightning flash may have one or more “strokes,” where the number of strokes refers to the number of times lightning travels over the same ionization channel. The number of strokes in a flash is referred to as the multiplicity of the lightning flash. Lightning “strikes” will be used to refer generically to either flashes or strokes. Cloud-to-cloud and intracloud lightning are not the focus of the present work, and unless specifically noted, “lightning” refers to cloud-to-ground lightning hereinafter.

A. Literature Survey

In an early study, Battan [12] employed simple visual observations of lightning strokes and correlated them to the number of inches of rain that fell during the same period and over the same area for thunderstorms in Arizona. He obtained the power-law relationship

$$n = 3.3r^{1.3} \quad (1)$$

where r is the number of inches of rain that fell during the observation period, and n is the number of lightning strokes during that observation period. The data exhibited significant scatter about (1). Kinzer [13] investigated cloud-to-ground lightning in Oklahoma thunderstorms and found that on a plot of n versus r , their data agreed reasonably well with Battan’s (1), although the scatter was large in this study as well.

Piepgrass *et al.* [14] investigated thunderstorms over Florida and found a linear relationship between n and the rain rate R , unlike the power law relationship of Battan [12]. The scatter about the linear fit was small, and the correlation was found to improve if a time lag was imposed between the lightning and rain data. The small degree of scatter about the linear fit that was observed by these authors occurred only when n and R were correlated for individual thunderstorms. Two storms were analyzed. For one storm the correlation was

$$n = 3 + 13R \quad (2)$$

while for the other storm the linear fit was

$$n = 21 + 26R \quad (3)$$

(a 5-min data-averaging interval was used in both cases). The slope in these two correlations differs by a factor of two and the y intercept by a factor of seven, showing how different these fits are. A much larger scatter would have resulted if the data from the two storms was pooled to create a single linear fit.

The degradation of the rain/lightning correlation when using datasets from more than one storm was demonstrated by Chèze and Sauvageot [15] also, who studied the relationship between radar-derived rain parameters and lightning in France. They fitted their data to a power law relation, correlating n to the fraction of the area covered by rainfall in the region considered. They found good correlation when individual storms were considered. However, when data from an entire season was considered, for example, the correlation was found to be much weaker.

Petersen and Rutledge [11] studied the relationship between cloud-to-ground lightning and convective rainfall over different portions of the continental U.S. and parts of the tropical western Pacific. These authors sought to improve correlations by considering data culled from very large spatial and temporal ranges, 10^5 km² and ~ 1 month, respectively. Here a reduction in scatter due to storm-to-storm fluctuations was sought by averaging over many of these storms. However, a unique relationship valid for all areas was not identified. An average rain yield was computed, where rain yield was defined as the rain flux (kilograms per second) divided by the flash rate (flashes per second), for each area. They found that this rain yield varied with location, attaining a value of 10^8 kg/flash in most of the midcontinental U.S., $\sim 6 \times 10^7$ kg/flash in the arid southwestern U.S. and in the tropics ranging from a continental value of 4×10^8 kg/flash to 10^{10} kg/flash in the tropical western Pacific Ocean. They found that using measured rain yields, they could produce a rainfall estimate that was accurate to within a factor of 2 of rain gauge measurements in the southern U.S., if hurricane affected month/locations were ignored. Note that by characterizing the lightning/rain relationship with a rain yield, these authors are implicitly assuming a linear relationship between R and n having a slope equal to the rain yield and a zero y intercept.

Tapia *et al.* [1] investigated rain and lightning in 22 Florida thunderstorms using WSR-88D radar data, rain gauge data, and NLDN data. They computed a rainfall–lightning ratio, identical to the rain yield of Petersen and Rutledge [11] and observed values ranging from 24×10^6 kg/flash to 365×10^6 kg/flash. They found this ratio was itself a function of the lightning intensity. The median value was 43×10^6 kg/flash.

Ezcurra *et al.* [16] investigated rain in several areas of Spain, computing the rain volume per lightning stroke occurring over three $20 \text{ km} \times 20 \text{ km}$ regions, each centered on a weather station. The volume of rain per lightning flash was computed, and large variations were observed between the three locations. Differences between oceanic and continental storms were also documented.

Zhou *et al.* [17] investigated lightning and rain in the Gansu province of the Peoples Republic of China. Rain was measured using a dual-polarization radar. They found a relationship between R and n

$$R = 1.69 \ln n - 0.27 \quad (4)$$

with a correlation coefficient of 0.86. However, this relation was obtained from only two days of observations.

The above studies seek to correlate a characteristic of the rain rate to a single characteristic of lightning. A smaller number of authors have sought to correlate rain to two lightning parameters. For example, Sheridan *et al.* [18] correlated regional mean precipitation (PCPN) to the measured lightning flash density (MGFD) and positive lightning flash density (PGFD) in six regions in the southcentral U.S. They first correlated their data according to the equation

$$\text{PCPN} = b_0 + b_1 \text{MGFD} \quad (5)$$

and then correlated their data using the equation

$$\text{PCPN} = b_0 + b_1 \text{MGFD} + b_2 \text{PGFD}. \quad (6)$$

They found significant improvement in the quality of the regression when (6) was used as opposed to (5) at all six measurement locations.

Seity *et al.* [19] also correlated rain to two lightning parameters. These authors analyzed lightning and rain during 21 stormy days in a coastal region of France. In their work they considered the polarity of the cloud-to-ground lightning strokes as well as the number of lightning strokes. Rain parameters were obtained from a meteorological radar, and the volume of rainfall per lightning flash RV was computed. RV was correlated to the fraction of lightning flashes having a positive polarity, and a linear relationship was found

$$RV = 6.87p + 8.73 \quad (7)$$

where RV is in units of $10^3 \text{ m}^3/\text{flash}$, and p is the percent of cloud-to-ground flashes having a positive polarity. This analysis was culled from a total of ten days for which the rain was of a nonfrontal type. For all but two of those days $p < 10\%$. The use of (7) in obtaining R requires the measurement of two parameters, p the fraction of positive lightning strokes, which provides RV from (7), and then n the number of strokes (over a defined area), which permits computation of the total volume of rainfall from the product ($RV \times n$).

Soula and Chauzy [20] performed a study similar to that of Seity *et al.* [19] using data obtained during four days in Paris, France, when convective storms were observed. Rain was measured by radar and converted to rain rate using a Z – R relationship. The results of these authors supported the work of Seity *et al.* [19]. They obtained the relationship

$$RV = 6.18p + 38.15 \quad (8)$$

where the definitions of the variables in (8) are identical to those in (7). Data for stratiform rain were not considered in this study.

It is interesting to note that in the studies cited above, the characteristics of rain that are correlated to lightning are bulk parameters such as the overall rain rate R , rain mass, or rain volume. Investigations that correlate, for example, the statistics of raindrop size, to lightning characteristics are lacking. While the ultimate goal of studies of the type cited above is to develop a method whereby R can be obtained from lightning measurements, it may nevertheless be useful to determine how specific characteristics of rainfall, such as drop size statistics, are related

to lightning. As will be demonstrated below, such statistics reveal information regarding the characteristics of storms. Hence, a method which can relate the statistics of raindrop size to lightning may be useful in the long-term development of a strategy for remotely measuring R using lightning. For example, while it may be difficult to directly correlate R to lightning strike density, it may be feasible to relate lightning to a characteristic of the raindrop size distribution. This in combination with a radar measurement, for example, could result in an effective remote sensing method for R .

A description of the raindrop size distribution is now presented.

B. Drop Size Distribution

The distribution of raindrop sizes is referred to as the drop size distribution (DSD) or $N(D)$. It is the number of drops per unit volume, for each drop size, and is related to the rain rate R via the integral

$$R = \frac{\pi}{6} \int_0^{\infty} N(D) D^3 v(D) dD \quad (9)$$

where v is the terminal velocity of the drop and D is the equivalent diameter of a spherical drop having the same volume as the raindrop. Hence, once $N(D)$ is known, R is easily computed.

The DSD is typically modeled as an exponential function. The exponential form originally suggested by Marshall and Palmer [21] is

$$N(D) = N_0 e^{-\Lambda D} \quad (10)$$

where N_0 and Λ are two unknown parameters. Once (N_0, Λ) are known, a functional form for the DSD can be written using (10) and then substituted into (9) to obtain R . Presented in this way, R is a function of two variables, N_0 and Λ .

Variations in the characteristics of rain due to storm type, geographical location, etc. are often revealed in the DSD. The sensitivity of the DSD to characteristics of the storm has been known since some of the earliest studies of the DSD. A seminal paper by Waldvogel [22] showed a distinct change in $N(D)$, specifically a jump in N_0 , when rain transitioned from the stratiform type to the convective type. More recently, Atlas *et al.* [23] demonstrated distinct changes in the shape of the DSD for convective and stratiform rain. These studies suggest that, if lightning has any relationship to the convective activity of a storm, then understanding how N_0 and Λ relate to lightning may provide some insight into a method for using lightning (most likely in combination with some other measurement) to sense R remotely. This is the motivation for the work presented here, where the relationship between (N_0, Λ) and n_s is investigated.

There are several aspects of rain and lightning that are important, but have not been discussed here. Latham *et al.* [24] have noted the importance of the ice-formation mechanism in the generation of lightning [25], [26] and developed relationships between rain rate and lightning strokes categorized according to the dominant glaciation mechanism. Such mechanisms are not considered here. Also, research exists on lightning over the ocean, such as that of Soriano and Pablo [27]. Here we focus solely on land-based results.

II. METHOD

Lightning data were obtained from the National Lightning Detection Network, a network of antennae on the continental U.S. providing geolocated data of lightning flashes. The NLDN is capable of identifying the time of arrival and location of lightning flashes with a detection probability of 80% to 90%. Geolocation is accurate to 500 m, on the average. Using data from this system permits a determination of the number of lightning strokes that fell within an arbitrarily sized box around any region of interest. NLDN data geolocates each lightning flash, providing the date, time, latitude, longitude, signal strength (kA), and the multiplicity of the flash which is the number of lightning strokes that were contained in the flash. In this work we counted the number of strokes that struck per hour, per square mile, n_s , computed over a prescribed square box centered on the Clemson Atmospheric Research Laboratory (CARL) where rain data were recorded (34.673° latitude, -82.886° longitude). The box sizes that were considered were 10, 20, 30, and 50 mi on a side. The number of strokes that struck within the box for each hour was compared to characteristics of the DSD, as determined by a disdrometer located at the center of the box.

In 1995, the NLDN was upgraded, resulting in improved detection efficiency. After the upgrade, it was noted that there was a disproportionately large increase in weak, positive flashes when compared to negative flashes. For example, Cummins *et al.* [28] noted that the increase in weak positive discharges was larger than the increase in weak negative charges. Wacker and Orville [29] made similar observations and in a companion paper developed a model of return stroke detection and presented an explanation of how intracloud (IC) flashes might explain the increase in weak positive flashes [30]. Cummins *et al.* [28] also suggest that the large increase in weak positive flashes is due to sensitivity to IC lightning. These authors suggest that positive flashes having a peak current <10 kA be rejected because of this. Rejection of <10 kA positive flashes has become common practice. In the present work such flashes are rejected also.

The DSD was obtained using a momentum disdrometer (Distromet RD-69 with attached ADA-90 analyzer) that recorded drop sizes in 20 bins ranging in size from 0.3–5.5 mm. The center values for each bin D_i and the bin widths w_i are presented in Table I. During a given rain event, data from the disdrometer were recorded in files as histograms for each minute. From these minute histograms, the discrete form of the DSD $N_i(D_i)$ was computed according to

$$N_i(D_i) = \frac{h_i(D_i)}{v_i A T w_i} \quad (11)$$

where $h_i(D_i)$ is the histogram of drops having diameter D_i , v_i is the terminal velocity of a drop having a diameter D_i , w_i is the bin width, A is the area of the disdrometer collection surface (50 cm²), and T is the duration of data collection in seconds. Data were averaged over hourly and daily periods. For hourly averages, h_i was obtained by summing over all minutes in the hour, and T in (11) was set to the number of minutes during the hour for which nonzero rain was recorded, multiplied by 60. When computing daily averages h_i was obtained by summing over all minutes in the day, and T was set to the number of

TABLE I
CENTER VALUE D_i AND BIN WIDTH w_i FOR EACH OF THE
20 DROP BINS RECORDED USING THE JOSS DISDRMETER

Bin	D_i (mm)	w_i (mm)
1	0.35	0.1
2	0.45	0.1
3	0.55	0.1
4	0.65	0.1
5	0.75	0.1
6	0.90	0.2
7	1.10	0.2
8	1.30	0.2
9	1.50	0.2
10	1.70	0.2
11	1.95	0.3
12	2.25	0.3
13	2.55	0.3
14	2.85	0.3
15	3.15	0.3
16	3.50	0.4
17	3.90	0.4
18	4.30	0.4
19	4.75	0.5
20	5.25	0.5

minutes during the day for which nonzero rain was recorded, multiplied by 60. Hence, $N_i(D_i)$ was always the DSD for time periods during which rain occurred, and hourly or daily averages of rain rate were not lowered due to periods during which rain was not falling. Hence, we are reporting the conditional rain rate, viz., the rain rate conditioned on $R > 0$. The formula used for terminal velocity v_i is that presented by Atlas *et al.* [31]

$$v = 9.65 - 10.3e^{-600D} \quad (12)$$

where D is in meters and v is in meters per second.

Once the DSD was computed, N_0 and Λ were calculated using the method described by Waldvogel, [22] where the water content W and radar reflectivity factor Z are computed according to

$$W = \frac{\pi}{6} \int_0^{\infty} N(D)D^3 dD \quad (13)$$

$$Z = \int_0^{\infty} N(D)D^6 dD \quad (14)$$

and then substituted into (15) and (16) to give N_0 and Λ

$$N_0 = \frac{1}{\pi} \left(\frac{6!}{\pi}\right)^{\frac{4}{3}} \left(\frac{W}{Z}\right)^{\frac{4}{3}} W = 446 \left(\frac{W}{Z}\right)^{\frac{4}{3}} W \quad (15)$$

$$\Lambda = \left(\frac{6!}{\pi}\right)^{\frac{1}{3}} \left(\frac{W}{Z}\right)^{\frac{1}{3}} = 6.12 \left(\frac{W}{Z}\right)^{\frac{1}{3}}. \quad (16)$$

Of course, the discrete DSD, $N(D_i)$ obtained from the disdrometer necessitated use of the discrete versions of (13) and (14)

$$W = \frac{\pi}{6} \sum_{i=1}^{20} N(D_i)D_i^3 w_i \quad (17)$$

$$Z = \sum_{i=1}^{20} N(D_i)D_i^6 w_i. \quad (18)$$

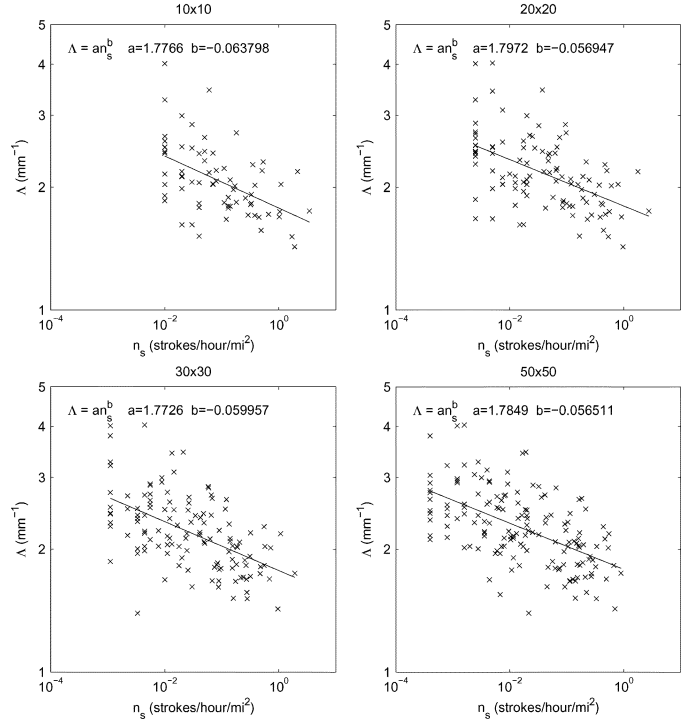


Fig. 1. Λ versus n_s for lightning data collected over a square region centered at CARL, having a size of (a) 10 mi \times 10 mi, (b) 20 mi \times 20 mi, (c) 30 mi \times 30 mi, and (d) 50 mi \times 50 mi. Λ and n_s were averaged over 1-h intervals.

Rain rate was also computed using the discrete version of (9)

$$R = \frac{\pi}{6} \sum_{i=1}^{20} N(D_i)D_i^3 v(D_i) w_i \quad (19)$$

where w_i is the disdrometer bin width, shown in Table I.

No attempt was made to select rain events based on the type of storm or front that was present.

III. RESULTS

Disdrometer data were collected during 3047 h during 215 days from January 1998 through September of 2003. NLDN data were available for each of these days. These data are presented after averaging over two time intervals: hourly and daily.

A. Hourly Averages

A total of 3047 h of disdrometer data were obtained. Of these 3047 h, 645 h were discarded because the histogram for that hour had only a single bin populated. Of the remaining 2402 h, the additional criterion was also applied that $R > 1$ mm/h and $n > 0$ where n is the number of lightning strokes in that hour. The hours remaining after application of these two criteria varied with box size since n had a greater chance of being nonzero for larger box sizes. For the 10 \times 10 mile box size, 86 h of data remained, 128 h for the 20 \times 20 mile box, 150 h for the 30 \times 30 mile box and 184 h for the 50 \times 50 mile box. The statistics for the $n = 0$ hours are described later in this section. Plots of Λ , N_0 , and R are presented in Figs. 1–3, respectively. These

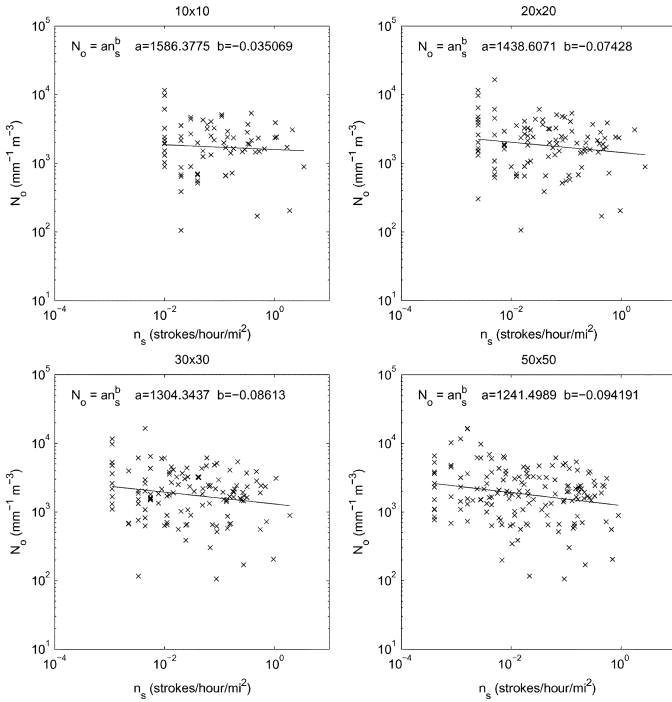


Fig. 2. N_0 versus n_s for lightning data collected over a square region centered at CARL, having a size of (a) 10 mi \times 10 mi, (b) 20 mi \times 20 mi, (c) 30 mi \times 30 mi, and (d) 50 mi \times 50 mi. N_0 and n_s were averaged over 1-h intervals.

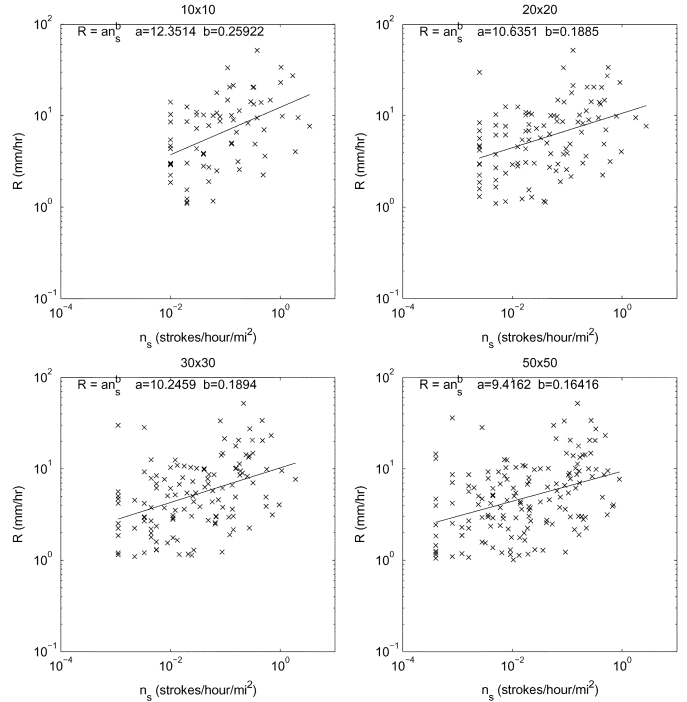


Fig. 3. R versus n_s for lightning data collected over a square region centered at CARL, having a size of (a) 10 mi \times 10 mi, (b) 20 mi \times 20 mi, (c) 30 mi \times 30 mi, and (d) 50 mi \times 50 mi. R was obtained from the disdrometer, located at CARL. R and n_s were averaged over 1-h intervals.

data are plotted against n_s which we define as the number of lightning strokes per hour scaled to the number of square miles over which lightning data were collected (strokes per hour per square mile). In each figure, data are presented for each of the four different box sizes considered. Note that the disdrometer data does not change with box size.

Power law fits of the form

$$\Lambda = a_1 n_s^{b_1} \tag{20}$$

$$N_0 = a_2 n_s^{b_2} \tag{21}$$

$$R = a_3 n_s^{b_3} \tag{22}$$

were obtained by doing a least squares fit to the logarithm of each of the data pairs, (Λ, n_s) , (N_0, n_s) , (R, n_s) . These fits are shown as solid lines in each of the plots presented in Figs. 1–3. Linear fits to these data were also obtained, but they performed poorly in comparison to the power law fits. The prefactors a and exponents b in each of these fits are included in the figure insets and are tabulated in Table II for each of the box sizes considered. The maximum-to-minimum range [(max-min)/avg] for each of the prefactors and exponents is presented in the last line of this table. This range is smaller for Λ than for either N_0 or R , indicating greater sensitivity to box size of N_0 and R for these hourly averages.

B. Daily Averages

The scatter is significant for the data presented in Figs. 1–3. Part of the reason for this is that many of the hours for which data were collected were hours where R was small, a condition which creates a DSD that is not smooth and results in er-

TABLE II
COEFFICIENTS FOR THE POWER LAW FITS DEFINED IN (20)–(22). DATA ARE AVERAGED OVER HOURLY INTERVALS PRIOR TO CURVE FITTING. a AND b ARE THE PREFACTORS AND EXPONENTS, RESPECTIVELY, FOR: 1) THE Λ FIT; 2) FOR THE N_0 FIT; AND 3) FOR THE R FIT. THE LAST ROW IN THE TABLE PRESENTS THE MAXIMUM TO MINIMUM RANGE FOR EACH OF THE EMPIRICAL CONSTANTS PRESENTED

Box Size (miles)	a_1	b_1	a_2	b_2	a_3	b_3
10	1.7766	-0.0638	1586.4	-0.0351	12.35	0.2592
20	1.7972	-0.0569	1438.6	-0.0743	10.66	0.1885
30	1.7726	-0.0600	1304.3	-0.0861	10.24	0.1894
50	1.7849	-0.0565	1241.5	-0.0942	9.416	0.1642
Max-Min Range	1.4%	12.1%	24.3%	91.4%	27.0%	44.9%

atic values for Λ and N_0 . To reduce the scatter, n_s , Λ , N_0 , and R were recomputed over 24-h intervals. The 215 days of data were subjected to the following criteria: 1) the average daily rain rate was >1 mm/h; 2) more than one bin was populated in the daily histogram; 3) at least one lightning stroke occurred during the day. The number of days satisfying these criteria was: 47 days for the 10 mi \times 10 mi box size, 50 days for the 20 mi \times 20 mi box size, 57 days for the 30 mi \times 30 mi box size, and 67 days for the 50 mi \times 50 mi box size. The plots of Λ versus n_s , N_0 versus n_s , and R versus n_s for these daily averaged data are presented in Figs. 4–6, respectively. In these figures, n_s is the number of lightning strokes per hour per square mile, averaged over one day. The power law fits to the data are of the same form as for the hourly case (20)–(22), and values of a and b for each of the variables plotted are presented in Table III, along with the maximum-to-minimum range in a and b for each box size.

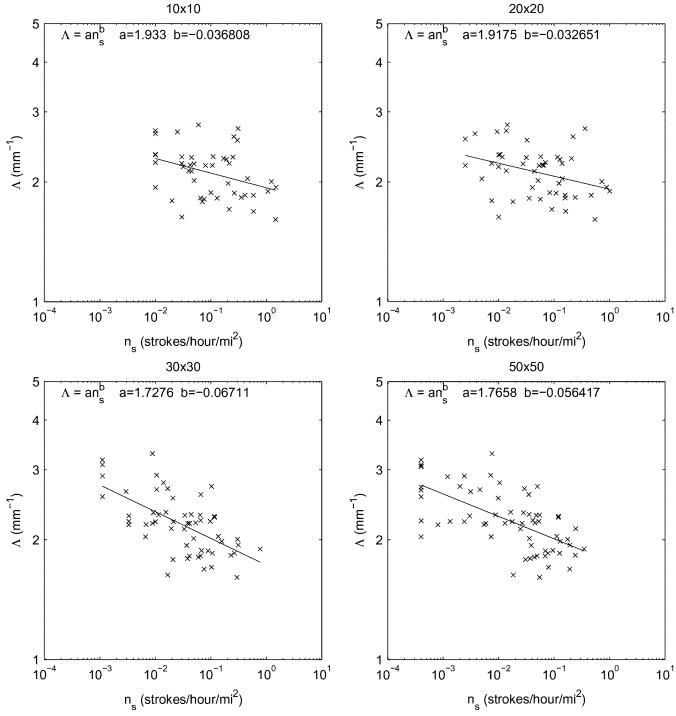


Fig. 4. Λ versus the number of lightning strokes per hour. Λ and n_s were averaged over a 24-h period. The lightning strokes were collected within a square area centered at CARL of size (a) 10 mi \times 10 mi, (b) 20 mi \times 20 mi, (c) 30 mi \times 30 mi, and (d) 50 mi \times 50 mi.

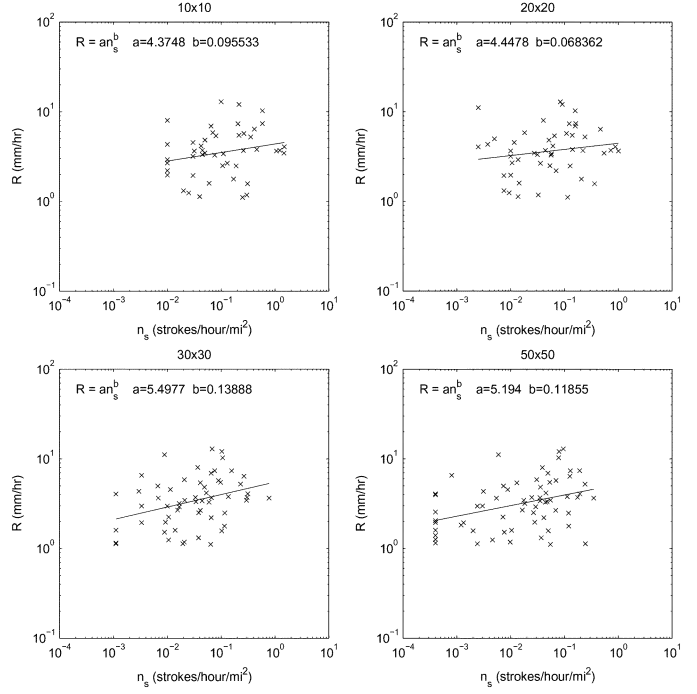


Fig. 6. R versus the number of lightning strokes per hour. R and n_s were averaged over a 24-h period. The lightning strokes were collected within a square area centered at CARL of size (a) 10 mi \times 10 mi, (b) 20 mi \times 20 mi, (c) 30 mi \times 30 mi, and (d) 50 mi \times 50 mi.

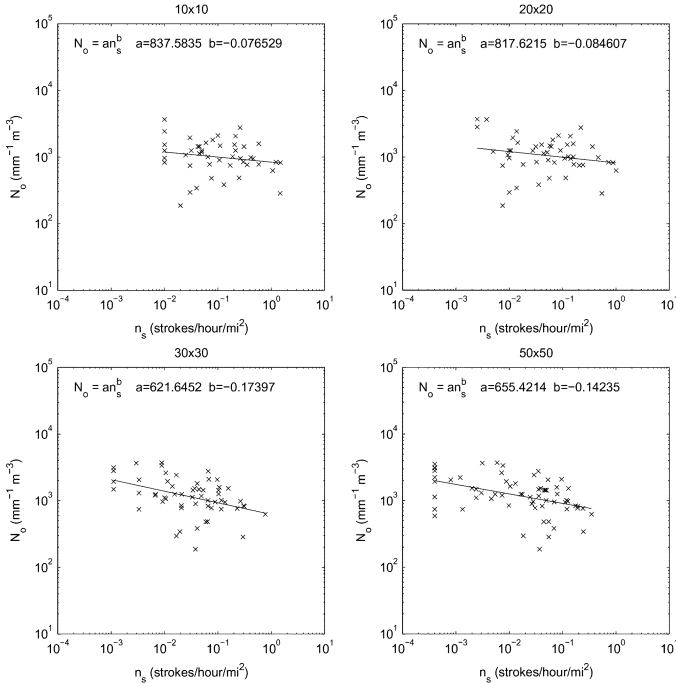


Fig. 5. N_0 versus the number of lightning strokes per hour. N_0 and n_s were averaged over a 24-h period. The lightning strokes were collected within a square area centered at CARL of size (a) 10 mi \times 10 mi, (b) 20 mi \times 20 mi, (c) 30 mi \times 30 mi, and (d) 50 mi \times 50 mi.

Averaging over a day decreases the scatter in the data as shown in Table IV. It also increases the maximum-to-minimum range in the prefactors and exponents, indicating a somewhat greater sensitivity to box size when averaging over an entire day.

C. Polarity Results

As noted in Section I, Seity *et al.* [19] and Soula and Chauzy [20] were able to correlate the volume of rain per lightning flash, to the fraction of lightning flashes having a positive polarity. We take a similar approach here by correlating R/n_s , the rain rate scaled by the number of strokes per hour per square mile, to the fraction of positive polarity strokes in the region considered, p . These data are plotted in Fig. 7, averaged over one-day intervals. A power law correlation between R/n_s and p provided a poor fit to the data. A much better result was obtained by using an exponential fit of the form

$$\frac{R}{n_s} = a_4 e^{b_4 p}. \quad (23)$$

This function fits the data reasonably well. However, there is significantly more scatter than observed by Seity *et al.* [19] and Soula and Chauzy [20].

For all of the lightning data considered, p was relatively constant with box size, having an average value of 5.3% for the 10 mi \times 10 mi box size, 5.7% for the 20 mi \times 20 mi box, 6.1% for the 30 mi \times 30 mi box, and 5.5% for the 50 mi \times 50 mi box.

D. Zero Lightning Data ($n_s = 0$)

Histograms are presented in Fig. 8 for R , N_0 , and Λ averaged over 1-h intervals for hours where $n_s = 0$. These provide a picture of the data excluded from Figs. 1–3 due to a $n_s = 0$ condition. These histograms did not change significantly with box size, and only the 10 mi \times 10 mi box size is shown here. These histograms show that for these zero lightning hours, the rain rate

TABLE III
COEFFICIENTS FOR THE POWER LAW FITS DEFINED IN (20)–(22) FOR DATA AVERAGED OVER A 24-h PERIOD. a AND b ARE THE PREFACTORS AND EXPONENTS, RESPECTIVELY, FOR: 1) THE Λ FIT; 2) FOR THE N_0 FIT; AND 3) FOR THE R FIT. THE LAST ROW IN THE TABLE PRESENTS THE MAXIMUM TO MINIMUM RANGE FOR EACH OF THE EMPIRICAL CONSTANTS PRESENTED

Box Size (miles)	a_1	b_1	a_2	b_2	a_3	b_3
10	1.9330	-0.0368	837.6	-0.0765	4.3748	0.0955
20	1.9175	-0.0326	817.6	-0.0846	4.4478	0.0684
30	1.7276	-0.0671	621.6	-0.1740	5.4977	0.1389
50	1.7658	-0.0564	655.4	-0.1424	5.1940	0.1185
Max-Min Range	11.2%	69.2%	29.6%	77.8%	22.7%	68.0%

TABLE IV
ROOT MEAN SQUARE DEVIATION OF DATA FROM THE EXPONENTIAL FITS PRESENTED IN FIGS. 1–6 FOR THE 50 mi \times 50 mi BOX SIZE OF Λ , N_0 , and R

	rms
Λ (hourly)	0.4185 mm ⁻¹
N_0 (hourly)	2556 mm ⁻¹ m ⁻³
R (hourly)	7.700 mm/hr
Λ (daily)	0.3183 mm ⁻¹
N_0 (daily)	797.3 mm ⁻¹ m ⁻³
R (daily)	2.574 mm/hr

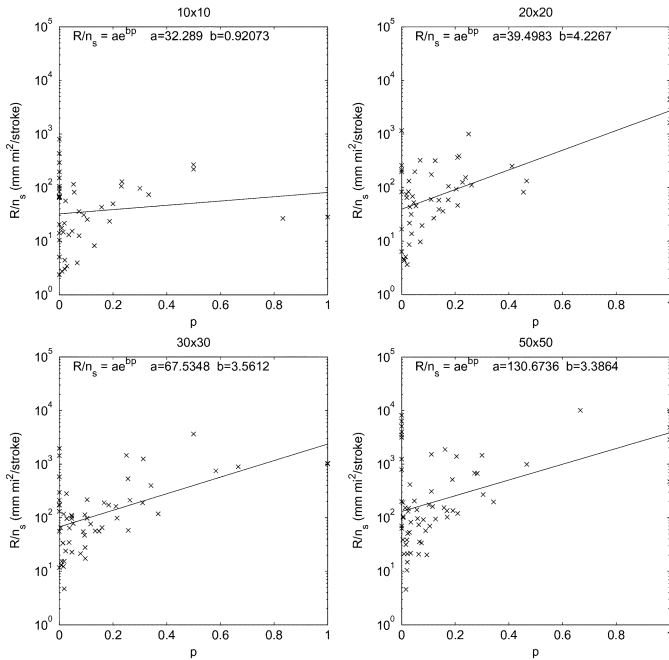


Fig. 7. R/n_s plotted against p , the fraction of cloud-to-ground lightning strokes having positive polarity. Data were acquired over a box size of (a) 10 mi \times 10 mi, (b) 20 mi \times 20 mi, (c) 30 mi \times 30 mi, and (d) 50 mi \times 50 mi.

tended to be small, as was the value of N_0 . The distribution of Λ for these zero lightning hours peaks at about 3 mm⁻¹.

IV. DISCUSSION

An important observation regarding the results presented above concerns the relative constancy of the values of a and b for Λ . Regardless of the box size, duration of averaging, or polarity, $a_1 \sim 1.8$ – 1.9 and $b_1 \sim -0.04$ to -0.06 , with few exceptions. The values of a and b for N_0 and R display much greater variation, particularly with regard to the duration of averaging. This suggests that the slope of the DSD, can be confidently predicted by a power law function of n_s even if

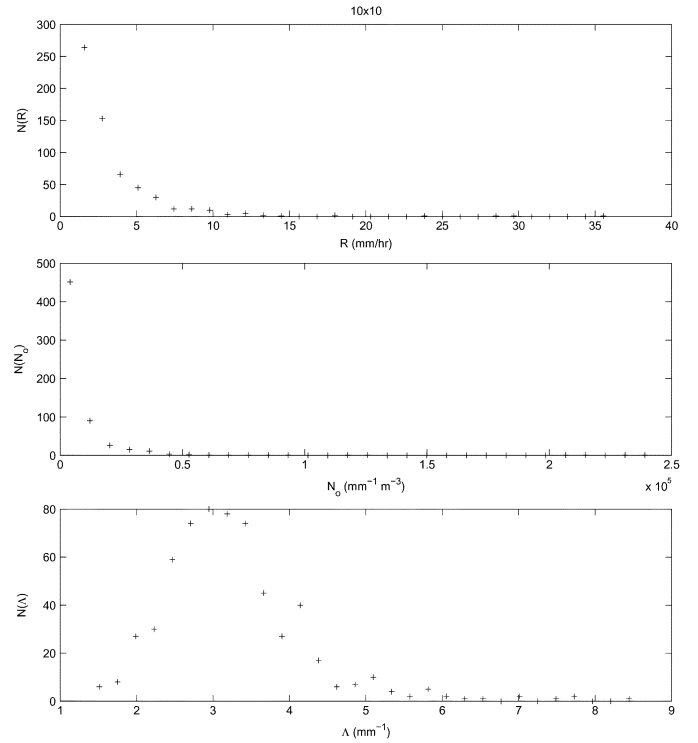


Fig. 8. Histograms of (a) R , (b) N_0 , and (c) Λ obtained from the disdrometer for hours where $n_s = 0$. The box size for lightning detection was 10 mi \times 10 mi, and hourly averages were used. Note that in this figure, $n_s = 0$ means no lightning at all. Hence, even hours that only had positive strokes with a peak current < 10 kA were not included in these histograms.

n_s is measured over areas or averaging periods of variable magnitude.

A second important observation is that the variables R , Λ , and N_0 all are well-fit by power law correlations. The variable R/n_s is best fit by an exponential correlation to p . A linear correlation performed poorly in all of these cases.

The data presented in the previous section suggest three methods by which R can be extracted from n_s .

- 1) First, by simply correlating R to n_s , as done in Fig. 6.
- 2) Second, using the DSD parameters Λ and N_0 , presented in Figs. 4 and 5. In this method, for a given value of n_s , both Λ and N_0 are extracted, and R computed according to (9) and (10).
- 3) The third method is to use the correlation between R/n_s and p . Here, p is used to obtain R/n_s , and then R is obtained by multiplying by n_s .

Each of these three methods was used to predict R . The daily averaged data were used, and for each day, the measured value of n_s was used to obtain a predicted value of R . For each method,

TABLE V
RMS DEVIATION OF RAIN RATE PREDICTED BY EACH CORRELATION METHOD COMPARED TO THE ACTUAL RAIN RATE. THE "SCALED RMS" IS THE RMS DEVIATION SCALED TO THE OVERALL AVERAGE RAINRATE. STATISTICS OBTAINED FOR THE 50 mi \times 50 mi BOX SIZE

Method	RMS deviation (mm/hr)	scaled RMS
(1) R versus n_s	2.57	0.67
(2) Λ and N_0 versus n_s	2.61	0.68
(3) R/n_s versus p	10.5	2.73

the root mean square (rms) deviation of the predicted value from the actual value was computed. The resulting rms deviations are presented in Table V along with the rms deviation scaled to the overall mean rainfall rate for this data. This table presents results for only the 50 mi \times 50 mi box size. The results show similar performance by methods #1 and #2 showing that the correlation between R and n_s and R obtained from DSD parameters and n_s is comparable, differing by less than 2%. This is as expected, since (N_0, Λ) are related to R via (9). The correlation of R obtained from the R/n_s versus p correlation was much worse. The recorded rainrates varied from 1–50 mm/h in this study.

The good performance of methods #1 and #2 presented in Table V seems to suggest that earlier attempts to obtain a correlation between R and n should have been more successful. However, it must be noted that most prior attempts sought to obtain a constant value for a ratio of R (or some variable related to R , such as mass flux) to n , implicitly seeking a linear correlation of R to n . The relationship used in methods #1 and #2 employs the power-law relationship presented in (20)–(22). Of the research cited in Section I, only Battan [12] sought a power law relationship between rain rate and lightning characteristics.¹ Hence, an important result of this work is that correlations between lightning characteristics and rainfall may be best sought for as power law correlations, rather than linear correlations.

It is unclear why method #3 performed so poorly, in light of the excellent performance documented by Seity *et al.* [19] and by Soula and Chauzy [20]. Perhaps this is due to the very small number of data points that were obtained by these authors under high p conditions. Seity *et al.* [19] had only two data points where $p > 0.1$ and Soula and Chauzy [20] reported only six data points where $p > 0.1$. The present study had a significantly larger number of large- p events suggesting that the correlation may change as p increases. Additionally, Seity *et al.* [19] considered only nonfrontal situations, and Soula and Chauzy [20] considered only convective systems, while no prefiltering of rain events was undertaken in the present work. Another possible reason for the difference between the present results and those of Seity *et al.* [19] and Soula and Chauzy [20] concerns the sensitivity of the NLDN array. As noted in Section I, the 1995 upgrade of the NLDN resulted in increased sensitivity and a believed misinterpretation of some IC strokes as low peak current positive amplitude strokes. To account for this, it is now common practice to reject positive strokes having a peak current < 10 kA. This practice has been done in the present study as well where 68%, 59%, 53%, and 49% of the positive strokes were eliminated for the 10 \times 10 mile, 20 \times 20 mile, 30 \times 30 mile, and

50 \times 50 mile box sizes, respectively. In the current NLDN configuration, the spacing of sensors is particularly high over the region where the present measurements were obtained. In fact, as noted by Orville and Huffines [32], sensor density peaks in the western Carolinas, where the present measurements were obtained. Moreover, these authors found that positive flashes having a peak current < 10 kA also peaked over the region where the current measurements were obtained. The increased sensitivity in the present work may mean that some IC flashes manifest themselves as cloud-to-ground flashes having peak currents that are greater than 10 kA in the western Carolinas, where sensitivity is higher than other parts of the network. If this is the case, it would explain the larger values of p observed here, compared with the work of Seity *et al.* [19] and Soula and Chauzy [20], and may also explain the poorer performance of the R/n_s versus p correlation.

Although Λ and N_0 provide a direct connection to R via (9), a better qualitative understanding of a rain event can be obtained from the related variables N_T and D_0 , the number of drops per unit volume and the median drop diameter, respectively. These variables are related to Λ and N_0 via

$$N_T = \frac{N_0}{\Lambda} \quad (24)$$

$$D_0 = \frac{3.67}{\Lambda}. \quad (25)$$

Substituting the power law scaling for Λ and N_0 [(20) and (21)] into (24) and (25) gives

$$N_T = \frac{a_2 n_s^{b_2 - b_1}}{a_1} \quad (26)$$

$$D_0 = \frac{3.67}{a_1 n_s^{b_1}}. \quad (27)$$

Substituting values for a_1, a_2, b_1 , and b_2 , obtained for the 50 mi \times 50 mi box size and 24-h averaging (Table III), results in

$$N_T = 371.2 n_s^{-0.086} \quad (28)$$

$$D_0 = 2.078 n_s^{0.0564}. \quad (29)$$

Values for N_T and D_0 were obtained by substituting typical values for n_s into (28) and (29), and the results are presented in Table VI. These numbers are typical of what to expect for Southeastern, summertime, convective rainfall where the predominant precipitation modification below cloud base should be collision-coalescence in the presence of high humidity. In such a case, there would be little loss of rain water due to evaporation in the fall of raindrops from cloud base to the surface. As coalescence decreases the numbers of drops per unit volume, there would be a consequent increase in mean raindrop size. If n_s is indeed a measure of storm severity, as we postulate herein, it would be expected that this effect would be more pronounced in storms with greater n_s , and that is what is displayed in Table VI.

Clearly, lightning cannot be used alone to measure R remotely, since there can be finite rainfall and variation in rainfall when $n_s = 0$. Hence, future application of the work presented here would most likely bear fruit by combining the parameterization of Λ and n_s with a radar method. Λ shows the greatest stability in the correlation to n_s with respect to the duration of

¹Chèze and Sauvageot [15] employed a power law relationship as well, but this was between n and the fraction of the area covered by rainfall.

TABLE VI
VALUES OF N_T AND D_0 FOR TYPICAL VALUES OF n_s

n_s	N_T (drops/m ³)	D_0 (mm)
10^{-4}	820	1.24
10^{-3}	672	1.41
10^{-2}	552	1.60
10^{-1}	453	1.83

averaging (daily versus hourly) and the box size over which averaging of the lightning strikes occurred, while N_0 shows less stability in this regard. This gives basically one parameter of the DSD which may be obtained robustly from n_s . Since two are required, a logical choice for a second would be the radar reflectivity. A procedure whereby this might be employed is suggested in the work of Testud *et al.* [33] where a method is presented for obtaining Z - R relationships once a value is obtained for N_0 . These authors show that

$$Z = AN_0^{-0.5}R^{1.5} \quad (30)$$

where A is dependent on the shape of the DSD and was found not to vary significantly (at least compared to variations in N_0). Hence, obtaining N_0 using the results obtained herein, and using (30) with an appropriate value for A , one obtains a Z - R relationship which would allow more accurate measurement of R from a single polarization radar measurement of Z , for example. Hence, through the combination of a single polarization radar measurement of Z and measurement of n_s via the NLDN, for example, one obtains a hybrid two-parameter measurement of R . Testud *et al.* [33] present an equation similar to (30) where N_0 is replaced by D_m , the mean volume diameter, which is related to Λ via

$$D_m = 4/\Lambda \quad (31)$$

for an exponential DSD. Hence, a Z - R relationship could also be obtained from the more stable Λ versus n_s correlations developed in this work.

Another possible future use of the work that was presented here concerns dual-polarization radars. The dual-polarization radar measurement of R relates the horizontal and vertical radar reflectivities (η_h, η_v) to (N_0, Λ) using electromagnetic scattering theory [34]. Once (N_0, Λ) are obtained, R is computed using (9). For these radars, the rain measurement problem is well-posed: there are two unknowns (N_0, Λ) and two measurements (η_h, η_v). However, even in this case, finite noise, calibration errors, and other sources of error can make inaccurate the value of N_0 and/or Λ that one obtains from η_h and η_v . Hence, it is possible that by using the relationship between Λ and n_s presented herein to overdetermine the problem, might improve rain rate retrievals when problems exist with either the η_h or η_v measurement.

Finally, the addition of another measurable to η_h and η_v might allow use of more sophisticated three-parameter models of the DSD. For example, Ulbrich and Atlas [35] demonstrated that actual DSDs could be more realistically represented using a gamma function of the form

$$N(D) = N_0 D^\mu e^{-\Lambda D} \quad (32)$$

where the three unknown parameters are (N_0, Λ, μ). Although Ulbrich [36] also showed that N_0 and μ could be empirically related, it is true nevertheless that an additional measurable would permit a complete three-parameter measurement of the DSD increasing the accuracy of R retrievals. It is possible that μ might be related to some characteristic of lightning and N_0 and Λ could be obtained from a dual-polarization radar, permitting a three-parameter measurement of R .

V. CONCLUSION

Attempts to correlate R, Λ , and N_0 to n_s using a power law fit were successful and suggest that this type of fit is more useful than a linear fit. The correlation of Λ to n_s was particularly stable, being insensitive to the averaging interval and the box size over which lightning data were collected. Parameterizing R directly to n_s was found to work just as well as parameterizing Λ and N_0 to n_s and then computing R . The polarity of the lightning stroke, while related to R , was not found to be particularly useful in improving the relationship between R and lightning. These results suggest that lightning by itself may be most effectively used to measure R , if it is combined with some other measurement such as a single-polarization radar to create a hybrid two-parameter method.

ACKNOWLEDGMENT

NLDN data were provided by the NASA Lightning Imaging Sensor (LIS) instrument team and the LIS data center via the Global Hydrology Resource Center located at the Global Hydrology and Climate Center, Huntsville, AL, through a license agreement with Global Atmospheric, Inc.

REFERENCES

- [1] A. Tapia, J. A. Smith, and M. Dixon, "Estimation of convective rainfall from lightning observations," *J. Appl. Meteorol.*, vol. 37, pp. 1497–1509, 1998.
- [2] D. Smith, K. Eack, J. Harlin, M. J. Heavner, A. R. Jacobson, R. S. Massey, X. M. Shao, and K. C. Wiens, "The Los Alamos Sferic Array: A research tool for lightning investigations," *J. Geophys. Res.*, vol. 107, 2002. DOI 10.1029/2001JD000502.
- [3] R. J. Thomas, P. R. Krehbiel, W. Rison, S. J. Hunyady, W. P. Winn, T. Hamlin, and J. Harlin, "Accuracy of the Lightning Mapping Array," *J. Geophys. Res.*, vol. 109, p. D14207, 2004.
- [4] H. J. Christian, K. T. Driscoll, S. J. Goodman, R. J. Blakeslee, D. A. Mach, and D. E. Buechler, "The Optical Transient Detector (OTD)," in *Proc. 10th Int. Conf. Atmospheric Electricity*, Osaka, Japan, 1996, pp. 368–371.
- [5] H. J. Christian, R. J. Blakeslee, S. J. Goodman, D. A. Mach, M. F. Stewart, D. E. Buechler, W. J. Koshak, J. M. Hall, W. L. Boeck, K. T. Driscoll, and D. J. Boccippio, "The Lightning Imaging Sensor," in *Proc. 11th Int. Conf. Atmospheric Electricity*, Guntersville, AL, 1999, pp. 746–749.
- [6] H. J. Christian, "Optical detection of lightning from space," in *Proc. 11th Int. Conf. Atmospheric Electricity*, Guntersville, AL, 1999, pp. 715–718.
- [7] J. Simpson, R. F. Adler, and G. R. North, "A proposed Tropical Rainfall Measuring Mission (TRMM) satellite," *Bull. Amer. Meteorol. Soc.*, vol. 69, pp. 278–295, 1988.
- [8] J. Simpson, C. Kummerow, W. K. Tao, and R. F. Adler, "On the Tropical Rainfall Measuring Mission (TRMM)," *Meteorol. Atmos. Phys.*, vol. 60, pp. 19–36, 1996.
- [9] M. H. Davis, M. Brook, H. Christian, B. G. Heikes, R. E. Orville, C. G. Park, R. G. Roble, and B. Vonnegut, "Some scientific objectives of a satellite-borne lightning mapper," *Bull. Amer. Meteorol. Soc.*, vol. 64, pp. 114–119, 1983.

- [10] H. J. Christian, R. J. Blakeslee, and S. J. Goodman, "The detection of lightning from geostationary orbit," *J. Geophys. Res.*, vol. 94, pp. 13 329–13 337, 1989.
- [11] W. A. Petersen and S. A. Rutledge, "On the relationship between cloud-to-ground lightning and convective rainfall," *J. Geophys. Res.*, vol. 103, pp. 14 025–14 040, 1998.
- [12] L. J. Battan, "Some factors governing precipitation and lightning from convective clouds," *J. Atmos. Sci.*, vol. 22, pp. 79–84, 1965.
- [13] G. D. Kinzer, "Cloud-to-ground lightning versus radar reflectivity in Oklahoma thunderstorms," *J. Atmos. Sci.*, vol. 31, pp. 787–799, 1974.
- [14] M. V. Piepgrass, E. P. Krider, and C. B. Moore, "Lightning and surface rainfall during Florida thunderstorms," *J. Geophys. Res.*, vol. 87, pp. 11 193–11 201, 1982.
- [15] J.-L. Chèze and H. Sauvageot, "Area-average rainfall and lightning activity," *J. Geophys. Res.*, vol. 102, pp. 1707–1715, 1997.
- [16] A. Ezcurra, J. Areitio, and I. Herrero, "Relationships between cloud-to-ground lightning and surface rainfall during 1992–1996 in the Spanish Basque country area," *Atmos. Res.*, vol. 61, pp. 239–250, 2002.
- [17] Y. Zhou, X. Qie, and S. Soula, "A study of the relationship between cloud-to-ground lightning and precipitation in the convective weather system in China," *Ann. Geophys.*, vol. 20, pp. 107–113, 2002.
- [18] S. C. Sheridan, J. F. Griffiths, and R. E. Orville, "Warm season cloud-to-ground lightning-precipitation relationships in the south-central United States," *Weather Forecast.*, vol. 12, pp. 449–458, 1997.
- [19] Y. Seity, S. Soula, and H. Sauvageot, "Lightning and precipitation relationship in coastal thunderstorms," *J. Geophys. Res.*, vol. 106, pp. 22 801–22 816, 2001.
- [20] S. Soula and S. Chauzy, "Some aspects of the correlation between lightning and rain activities in thunderstorms," *Atmos. Res.*, vol. 56, pp. 355–373, 2001.
- [21] J. S. Marshall and W. M. Palmer, "The distributions of raindrops with size," *J. Meteorol.*, vol. 9, pp. 327–332, 1948.
- [22] A. Waldvogel, "The N_0 jump of raindrop spectra," *J. Atmos. Sci.*, vol. 31, pp. 1068–1078, 1974.
- [23] D. Atlas, C. W. Ulbrich, F. D. Marks, Jr., E. Amitai, and C. R. Williams, "Systematic variation of drop size and radar-rainfall relations," *J. Geophys. Res.*, vol. 104, pp. 6155–6169, 1999.
- [24] J. Latham, A. M. Blyth, H. J. Christian, Jr., W. Deierling, and A. M. Gadian, "Determination of precipitation rates and yields from lightning measurements," *J. Hydrol.*, vol. 288, pp. 13–19, 2004.
- [25] S. J. Goodman, D. E. Buechler, and P. D. Wright, "Lightning and precipitation history of a microburst-producing storm," *Geophys. Res. Lett.*, vol. 15, pp. 1185–1188, 1988.
- [26] J. E. Dye, J. J. Jones, W. P. Winn, T. A. Cerni, B. Gardiner, D. Lamb, R. L. Pitter, J. Hallett, and C. P. R. Saunders, "Early electrification and precipitation development in a small isolated Montana cumulonimbus," *J. Geophys. Res.*, vol. 91, pp. 1231–1247, 1986.
- [27] L. R. Soriano and F. De Pablo, "Analysis of convective precipitation in the western Mediterranean Sea through the use of cloud-to-ground lightning," *Atmos. Res.*, vol. 66, pp. 189–202, 2003.
- [28] K. L. Cummins, M. J. Murphy, E. A. Bardo, W. L. Hiscox, R. B. Pyle, and A. E. Pifer, "A combined TOA/MDF technology upgrade of the U.S. National Lightning Detection Network," *J. Geophys. Res.*, vol. 103, pp. 9035–9044, 1998.
- [29] R. S. Wacker and R. E. Orville, "Changes in measured lightning flash count and return stroke peak current after the 1994 U.S. National Lightning Detection Network upgrade. 1. Observations," *J. Geophys. Res.*, vol. 104, pp. 2151–2157, 1999.
- [30] ———, "Changes in measured lightning flash count and return stroke peak current after the 1994 U.S. National Lightning Detection Network upgrade. 2. Theory," *J. Geophys. Res.*, vol. 104, pp. 2159–2162, 1999.
- [31] D. Atlas, R. C. Srivastava, and R. S. Sekhon, "Doppler radar characteristics of precipitation at vertical incidence," *Rev. Geophys. Space Phys.*, vol. 2, pp. 1–35, 1973.
- [32] R. E. Orville and G. R. Huffines, "Cloud-to-ground lightning in the United States: NLDN results in the first decade, 1989–98," *Mon. Weather Rev.*, vol. 129, pp. 1179–1193, 2001.
- [33] J. Testud, S. Oury, R. A. Black, P. Amayene, and X. K. Dou, "The concept of "normalized" distribution to describe raindrop spectra: A tool for cloud physics and cloud remote sensing," *J. Appl. Meteorol.*, vol. 40, pp. 1118–1140, 2001.

- [34] R. J. Doviak and D. S. Zmija, *Doppler Radar and Weather Observations*. Orlando, FL: Academic, 1984.
- [35] C. W. Ulbrich and D. Atlas, "Assessment of the contribution of differential polarization to improve rainfall measurements," *Radio Sci.*, vol. 19, pp. 49–57, 1984.
- [36] C. W. Ulbrich, "Natural variations in the analytical form of the raindrop size distribution," *J. Climate App. Meteorol.*, vol. 22, pp. 1764–1775, 1983.



John R. Saylor received the B.S. degree from the State University of New York, Buffalo, the M.S. degree from the University of Minnesota, Minneapolis, and the Ph.D. degree from Yale University, New Haven, CT, in 1986, 1989, and 1993, respectively.

He was an NRC Postdoctoral Associate at the Naval Research Laboratory, Washington, DC and since 2000 has been an Assistant Professor in the Department of Mechanical Engineering, Clemson University. His research interests include lightning, rain, the optics of droplets, and the general area of

interfacial hydrodynamics.

Dr. Saylor is a member of the American Physical Society, the American Society of Mechanical Engineers, Sigma Xi, The Oceanography Society, the American Geophysical Union, and the American Meteorological Society.



Carl W. Ulbrich received the B.S. degree in mechanical engineering, the M.S. degree in physics, and the Ph.D. degree in physics from the University of Connecticut, Storrs, in 1960, 1962, and 1965, respectively.

He served as a Professor in the Department of Physics, Clemson University, Clemson, SC, until 1993 and then as Research Professor until 2003. He is currently an Emeritus Professor at Clemson. His research interests include radar meteorology and atmospheric physics.



James W. Ballentine received the B.S. degree from Clemson University, Clemson, SC, in 2004.



Justin L. Lapp received the B.S. degree from the Rose Hulman Institute of Technology, Terre Haute, IN, in 2004. He is currently pursuing the M.S. degree at Clemson University, Clemson, SC.